

# Journal Pre-proof

Electrochemically Manipulating the Redox State of 2,2',5,5'-Tetrahydroxybiphenyl as a New Organic Li-rich Cathode for Li-ion Batteries



Qihang Yu, Zeyi Yao, Jianyou Shi, Wu Tang, Chuan Wang, Di Li, Cong Fan

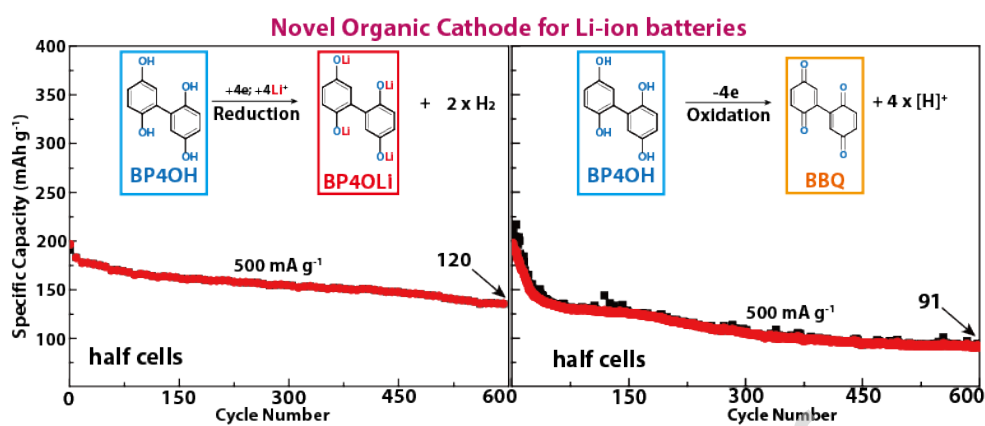
PII: S1566-1199(20)30047-1  
DOI: <https://doi.org/10.1016/j.orgel.2020.105661>  
Reference: ORGELE 105661  
To appear in: *Organic Electronics*  
Received Date: 10 January 2020  
Accepted Date: 12 February 2020

Please cite this article as: Qihang Yu, Zeyi Yao, Jianyou Shi, Wu Tang, Chuan Wang, Di Li, Cong Fan, Electrochemically Manipulating the Redox State of 2,2',5,5'-Tetrahydroxybiphenyl as a New Organic Li-rich Cathode for Li-ion Batteries, *Organic Electronics* (2020), <https://doi.org/10.1016/j.orgel.2020.105661>

This is a PDF file of an article that has undergone enhancements after acceptance, such as the addition of a cover page and metadata, and formatting for readability, but it is not yet the definitive version of record. This version will undergo additional copyediting, typesetting and review before it is published in its final form, but we are providing this version to give early visibility of the article. Please note that, during the production process, errors may be discovered which could affect the content, and all legal disclaimers that apply to the journal pertain.

© 2019 Published by Elsevier.

**Graphical abstract:** an organic molecule of 2,2',5,5'-tetrahydroxybiphenyl (BP4OH) with controllable redox state is firstly reported as the new cathode for Li-ion batteries.



# Electrochemically Manipulating the Redox State of 2,2',5,5'-Tetrahydroxybiphenyl as a New Organic Li-rich Cathode for Li-ion Batteries

Qihang Yu<sup>1+</sup>, Zeyi Yao<sup>1+</sup>, Jianyou Shi<sup>2+</sup>, Wu Tang<sup>1+</sup>, Chuan Wang<sup>1</sup>, Di Li<sup>1</sup> and Cong Fan<sup>1\*</sup>

1. School of Materials and Energy, University of Electronic Science and Technology of China (UESTC), Chengdu 611731, PR China

**E-mail:** fancong@uestc.edu.cn

2. Personalized Drug Therapy Key Laboratory of Sichuan Province, Department of Pharmacy, Sichuan Academy of Medical Sciences & Sichuan Provincial People's Hospital, Chengdu 610072, PR China

[+] These authors contributed equally to this work

**KEYWORDS:** 2,2',5,5'-tetrahydroxybiphenyl; in-situ synthesis; new organic cathodes; redox state; Li-ion batteries

**ABSTRACT:** For the first time, a small organic molecule of 2,2',5,5'-tetrahydroxybiphenyl (BP4OH) is synthesized as a new organic cathode for Li-ion batteries. After setting reduction in the 1<sup>st</sup> cycle in Li-ion half cells (reduction→oxidation), BP4OH can be in-situ transformed to its salt of lithium 2,2'-bis[benzene-1,4-bis(olate)] (BP4OLi) on Al foil. The resulting BP4OLi is a Li-rich organic cathode and exhibits very good cell performance. For example, the average capacity of ~155 mAh g<sup>-1</sup> for the BP4OLi electrode is realized during 600 cycles (500 mA g<sup>-1</sup>). On the other hand, after setting oxidation in the 1<sup>st</sup> cycle (oxidation→reduction), BP4OH can be in-situ tuned to its oxidized state of 2,2'-bis(1,4-benzoquinone) (BBQ). Interestingly, the resulting BBQ can be still redox-active and

show satisfactory cell performance. For instance, the average capacity of  $\sim 101 \text{ mAh g}^{-1}$  for the BBQ electrode can be obtained for 600 cycles ( $500 \text{ mA g}^{-1}$ ). This work reveals very interesting redox behaviors of organic electrodes.

## 1. INTRODUCTION

Due to the outstanding merits like high energy density and low cost, organic redox-active compounds have opened the new horizon for development of the next-generation rechargeable batteries, particularly for Li-ion batteries (LIBs) [1-6]. On the cathode side, organic moiety of 1,4-benzoquinone (BQ) with very clear two-electron mechanism can realize the maximum (max.) specific capacity of  $496 \text{ mAh g}^{-1}$  in LIBs, which is one of the best organic cathodes reported to date [7-12]. To be a qualified electrode material with Faraday mechanism, an organic electrode material must simultaneously possess stable reduced and oxidized states (redox couple) [12, 13]. And 1,4-benzoquinone (BQ) basically exists as oxidized state while its reduced state is the metal salt of [benzene-1,4-bis(olate)]<sup>2+</sup>, where the cation of the related metal salt is Li ion in LIBs [14]. Notably, both the reduced state [lithium benzene-1,4-bis(olate) (BP2OLi)] and the oxidized state (BQ) are highly stable in electrochemical environment.

To construct Li-ion full batteries, the redox state of a cathode must match with the redox state of an anode. For instance, BQ of oxidized state on the cathode side must be coupled with a material of reduced state on the anode side (such as Li metal) during battery fabrication [15-17]. Notably, the kinds of such reduced-state anodes are currently very scarce. On the other hand, the electron-rich organic anion moiety of [benzene-1,4-bis(olate)]<sup>2+</sup> is very sensitive to oxygen ( $\text{O}_2$ ), which makes [benzene-1,4-bis(olate)]<sup>2+</sup> and its derivatives air-unstable and difficult to purify at lab conditions. Currently, very few Li salts of [benzene-1,4-bis(olate)]<sup>2+</sup> and its derivatives have been

reported as the organic cathodes for LIBs [14, 18]. Notably, the Li salts of [benzene-1,4-bis(olate)]<sup>2+</sup> and its derivatives can be regarded as the Li-rich organic cathodes in LIBs [19].

In our previous study, we initially unveiled that the active proton (H<sup>+</sup>) in -COOH group of terephthalic acid (H<sub>2</sub>TP) could be electrochemically changed to hydrogen gas (H<sub>2</sub>) below certain reduction potential (vs. Li<sup>+</sup>/Li) in Li-ion half cells and thus the resulting -COOLi salt (Li<sub>2</sub>TP) was successfully realized [20]. Currently, there are very few reports that this effective strategy can be widely applied to -OH group of organic aromatic moieties [19]. In this article, we synthesized and initially used 2,2',5,5'-tetrahydroxybiphenyl (BP4OH) as the starting organic electrode material to prove that the aromatic -OH group could also be in-situ converted to lithium salt (-OLi group) through electrochemical synthesis. As a consequence, the resulting lithium 2,2'-bis[benzene-1,4-bis(olate)] (BP4OLi, C<sub>T</sub>=443 mAh g<sup>-1</sup>) could be in-situ employed as the Li-rich organic cathode for LIBs. For example, the resulting BP4OLi electrode could deliver the max. discharge capacity of ~432 mAh g<sup>-1</sup> with the average discharge potential of ~2.5 V (vs. Li<sup>+</sup>/Li) in LIBs. Consequently, an impressively high energy density (>1000 Wh kg<sup>-1</sup>) could be realized for the Li-rich BP4OLi.

More interestingly, we simultaneously proved that the oxidized state [2,2'-bis(1,4-benzoquinone), BBQ] of 2,2',5,5'-tetrahydroxybiphenyl (BP4OH) could also be in-situ synthesized above certain oxidation potential (vs. Li<sup>+</sup>/Li) in Li-ion half cells. Notably, four equivalents of active proton (H<sup>+</sup>) were released during the 1<sup>st</sup> oxidation process. And the in-situ formed BBQ could be used as the oxidized-state organic cathode in LIBs. Indeed, the BBQ electrode could still deliver the max. discharge capacity of 473 mAh g<sup>-1</sup> with the average discharge potential of ~2.5 V (vs. Li<sup>+</sup>/Li). And the average discharge capacity was ~204 mAh g<sup>-1</sup> for the BBQ electrode during 100 cycles (50 mA g<sup>-1</sup>).

## 2. Experimental section

**2.1 General information:** All reagents commercially available were used as received. For example, 1-bromo-2,5-dimethoxybenzene, (2,5-dimethoxyphenyl)boronic acid,  $\text{BBr}_3$  (boron tribromide) and polyacrylonitrile copolymer (La133) were from Shanghai Aladdin Bio-Chem Technology Co., LTD.. The carbon additives of CMK-3 and Super P (SP) were provided by XFnano CO., LTD..

**2.2 Synthesis of 2,2',5,5'-tetramethoxybiphenyl:** A mixture of 2-bromo-1,4-dimethoxybenzene (9.4 ml, 62.6 mmol), (2,5-dimethoxyphenyl)boronic acid (13.5 g, 74.2 mmol),  $\text{K}_2\text{CO}_3$  (12.0 g, 87.0 mmol), NaF (42 mg, 1 mmol) and tetrakis(triphenylphosphine)palladium(0) ( $\text{Pd}(\text{PPh}_3)_4$ , 5 mg) was dissolved in 120 ml 1,4-dioxane and 30 ml water under nitrogen atmosphere. The mixture was refluxed at 100 °C for 48h. After back to room temperature, 200 ml ethyl acetate was added and the mixture was washed three times with 100 ml water each. The organic layer was then separated and dried with  $\text{Na}_2\text{SO}_4$ . The product of 2,2',5,5'-tetramethoxybiphenyl was obtained by using column chromatography with the eluent of petroleum:ethyl acetate=5:1 (v:v) as a white crystalline solid (15.5 g, 56.6 mmol). The yield was 90%.  $^1\text{H}$  NMR (400 MHz, ppm,  $\text{CDCl}_3$ ,  $\delta$ ): 6.92-6.90 (d, J = 8.0 Hz, 2H), 6.88-6.87 (d, J = 4, 2H), 6.85-6.84 (m, 2H), 3.78 (s, 6H;  $\text{OCH}_3$ ), 3.73 (s, 6H;  $\text{OCH}_3$ ).

**2.3 Synthesis of 2,2',5,5'-tetrahydroxybiphenyl (BP4OH):** 1096 mg (4 mmol) 2,2',5,5'-tetramethoxybiphenyl was first dissolved in 40 ml anhydrous dichloromethane (DCM). After the solution was cooled down to 0 °C, 1.7 ml  $\text{BBr}_3$  (18 mmol) was slowly dropped into the solution [3]. After 4 hours, 5 ml deionized water was added and then the mixture was dried under diminished pressure. Afterwards, 40 ml ethyl acetate was added and the solution was washed three times by 50 ml water. The organic layer was separated and dried with  $\text{Na}_2\text{SO}_4$ . BP4OH was obtained by using column chromatography with the eluent of petroleum:ethyl acetate = 1:1 (v:v) as a white powder.

The yield was 90% (785 mg, 3.6 mmol).  $^1\text{H}$  NMR (400 MHz, ppm, DMSO): 8.74 (s, 2H; OH), 8.60 (s, 2H; OH), 6.72-6.68 (m, 2H), 6.58-6.54 (m, 4H).

**2.4 Preparation of BP4OH electrode:** The electrode was composited by BP4OH and CMK-3 with the optimized weight ratio of 4:5 after heavy attempts and the preparation details were as follows:

BP4OH was dissolved in tetrahydrofuran (THF) and CMK-3 was added to the BP4OH solution. After ultrasonic treatment for 30 min, the mixture was placed in oven to remove the solvent at 80 °C. Then BP4OH and CMK-3 composition was ground and evenly mixed before the addition of La133 and no further modifications were carried out. Due to the dissolution concern, the neat loading of BP4OH on Al foil was in the range of 1.2-1.6 mg cm<sup>-2</sup>.

**2.5 Preparation and test of Li-ion cells:** The composition slurry was casted on an Al foil (the Al foil was then punched into Al disk with diameter of 12 mm) and then dried in the vacuum oven at 60 °C for 24 h. In Li-ion half cells, the counter electrode was Li-metal slice; the electrolyte was 2 M lithium bis(trifluoromethane)sulfonamide (LiTFSI Shanghai Aladdin Bio-Chem Technology Co., LTD) in the mixture solvents of 1,3-dioxolane (DOL) and 1,2-dimethoxyethane (DME) with volume ratio of 1:1; and the separator was poly(propylene) (PP, Celgard 2400) membrane. All cells were assembled in the Ar-filled glove box. The galvanostatic charge-discharge tests and galvanostatic intermittent titration technique (GITT) were performed on a Land test system (CT2001A, China). Cyclic voltammograms (CVs) for half cells were tested at a scan rate of 0.1 mV s<sup>-1</sup> between 0.35 V and 3.7 V using the Bio-logic electrochemical workstation (VMP3-128). The electrochemical impedance spectroscopy (EIS) was measured by CHI660E electrochemical workstation with a frequency range from 0.01 Hz to 100 kHz.

### 3. Results and discussions

### 3.1 Synthesis and characterizations

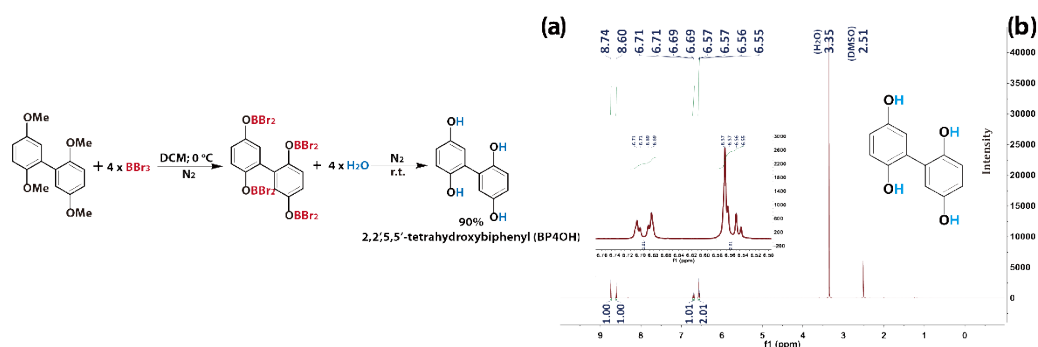


**Figure 1.** (a) The modified synthetic route for 2,2',5,5'-tetrahydroxybiphenyl (BP4OH); (b)  $^1\text{H}$  NMR of 2,2',5,5'-tetrahydroxybiphenyl (BP4OH).

As shown in **Figure 1a**, a modified synthetic route was developed to realize 2,2',5,5'-tetrahydroxybiphenyl (BP4OH) with gram scale by starting from 2,2',5,5'-tetramethoxybiphenyl [20]. See details in Experimental section. Impressively, the production yield of BP4OH was significantly improved from 34% to 90% after raising the temperature from  $-78\text{ }^\circ\text{C}$  to  $0\text{ }^\circ\text{C}$ . The organic molecules were well characterized by  $^1\text{H}$  NMR spectroscopy (**Figure 1b**) [21, 22].

### 3.2 Reduction $\rightarrow$ oxidation cycle

#### 3.2.1 CV Test

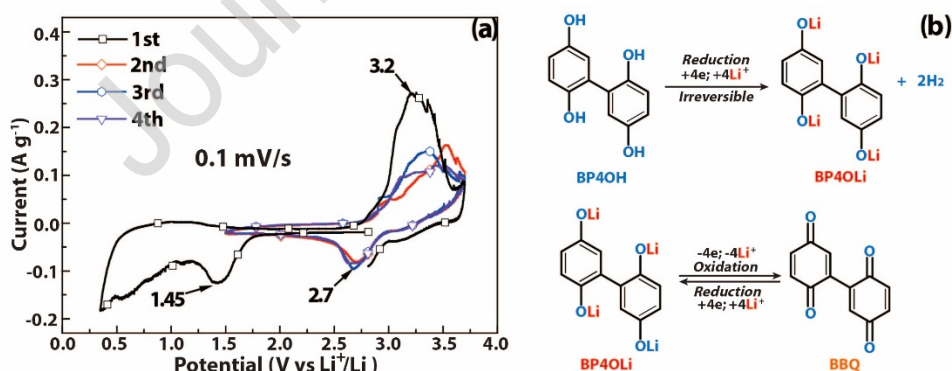


**Figure 2.** (a) CV curves of BP4OH from reduction $\rightarrow$ oxidation process in the 1<sup>st</sup> cycle. The scan rate was  $0.1\text{ mV s}^{-1}$ . The voltage window was 0.35–3.7 V in the 1<sup>st</sup> cycle and 1.5–3.7 V in the following cycles; (b) The detailed mechanism for the reduction $\rightarrow$ oxidation process of BP4OH.

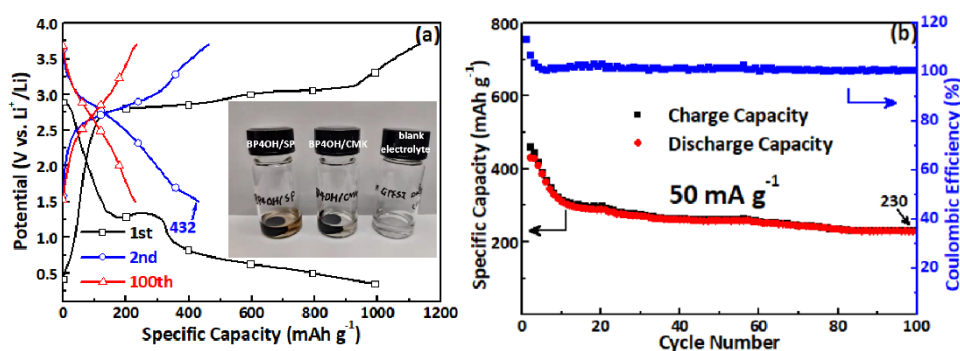
By setting reduction to 0.35 V during the 1<sup>st</sup> cycle, the cyclic voltammograms (CVs) were carried out for BP4OH in Li-ion half cells. And the cell fabrication details were demonstrated in

Experimental section. The electrode composition was prepared by BP4OH/Super P (SP)/binder with the weight ratio of 40:50:10, and the binder was optionally selected to be LA133. Importantly, the minimum potential of 0.35 V with cathodic scan direction in the 1<sup>st</sup> cycle was to confirm that the H<sup>+</sup> proton of BP4OH could get reduced to H<sub>2</sub> as well as the formation of a thick solid-electrolyte interface (SEI). The resulting CVs curves of BP4OH were shown in **Figure 2a**. In the 1<sup>st</sup> cathodic (reduction) scan, there was only one obvious reduction peak located at ~1.45 V (vs. Li<sup>+</sup>/Li). When the 1<sup>st</sup> reduction potential was below 1 V, a thick SEI was usually constructed by the side reactions of tiny impurities and decompositions of electrolytes. But in the back 1<sup>st</sup> anodic scan, one clear oxidation peak located at the relatively-high potential of ~3.2 V could be observed. Interestingly, in the 2<sup>nd</sup> cathodic scan, a new reduction peak appeared at ~2.7 V while the back oxidation peak in the 2<sup>nd</sup> scan still located at the high potential of ~3.5 V. Therefore, the reduction peak at ~1.45 V (vs. Li<sup>+</sup>/Li) should be the H<sup>+</sup> reduction from -OH group of BP4OH [19]. As a result, the related lithium 2,2'-bis[benzene-1,4-bis(olate)] (BP4OLi, C<sub>T</sub>=443 mAh g<sup>-1</sup>) could be in-situ synthesized on Al foil. Meanwhile, the reversible redox couple at ~2.7/3.2 V should be attributed to the electrochemical transformation between BP4OLi and its oxidized state (BBQ). Notably, BP4OLi could be more hardly dissolved when compared to the neutral BBQ molecule because of its four strong O-Li ionic bonds. Summarily, the detailed mechanism for the reduction→oxidation cycle of BP4OH was shown in **Figure 2b**.

### 3.2.2 Li-ion half cells

Subsequently, the cell performance based on BP4OH electrode was tested, where Super P as the carbon conductive additive was still used. However, the BP4OH/SP electrode only exhibited fair capacities in Li-ion half cells. The discharge capacity in the 2<sup>nd</sup> cycle was merely 335 mA h g<sup>-1</sup>

(50 mA g<sup>-1</sup>), along with quick capacity fading in the following cycles. Obviously, the fading was largely caused by the dissolution of BP4OH (inset of **Figure 3a**)[23]. After many attempts for electrode compositions, CMK-3 was chosen as the carbon additive, since the mesoporous CMK-3 with chemically-active sites could effectively absorb small organic molecules like BP4OH [3, 24-26]. Expectantly, the dissolution of BP4OH was obviously delayed by compositing with CMK-3. Basically, the different weight ratio of between BP4OH and CMK-3 has been tried in our previous study [27]. And only the case with the weight ratio of 4:5 could display the best battery performance since the full impregnation of small organic molecules into the CMK-3 scaffold. The charge-discharge curves of the BP4OH/CMK-3 electrode was shown in **Figure 3a**. In the 1<sup>st</sup> cycle, the specific discharge capacity for the resulting BP4OLi electrode was much higher than its theoretical capacity ( $C_T=443$  mAh g<sup>-1</sup>), since it contained the capacity contribution from the formation of solid-electrolyte interface (SEI) and the reduction capacity of  $H^+ \rightarrow H_2$ . Notably, the resulting BP4OLi/CMK-3 electrode delivered the improved discharge capacity of 432 mAh g<sup>-1</sup> in the 2<sup>nd</sup> cycle when compared to the one with Super P (335 mAh g<sup>-1</sup>@2<sup>nd</sup> cycle). The specific capacity contribution from CMK-3 was measured under the same conditions and estimated to be ~84 mAh g<sup>-1</sup> (~67 mAh g<sup>-1</sup> x 1.25). In addition, small organic molecules will occupy many chemically-active sites of CMK-3 [28, 29], thus indicating that the specific capacity contribution from CMK-3 should be less than ~84 mAh g<sup>-1</sup>.



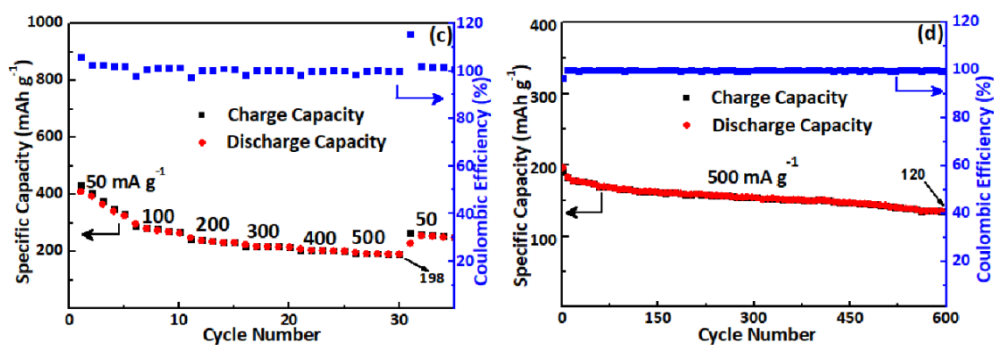


**Figure 3.** (a) The selected charge-discharge curves for BP4OLi electrode; (b) The 100 cycles for BP4OLi electrode at 50 mA g<sup>-1</sup>; (c) Rate performance of BP4OLi electrode; (d) The long cycles for BP4OLi electrode at 500 mA g<sup>-1</sup>.

Furthermore, the resulting BP4OLi/CMK-3 electrode exhibited the improved cycle stability at low current density. As shown in **Figure 3b**, the BP4OLi/CMK-3 electrode could fulfill the average capacity of ~266 mAh g<sup>-1</sup> during 100 cycles (test for one month at least) and still remained ~230 mAh g<sup>-1</sup> at the 100<sup>th</sup> cycle at a low current density of 50 mA g<sup>-1</sup>. However, the capacity of the BP4OLi/CMK-3 electrode declined slowly in the first few cycles for the dissolution problem. Indeed, the BP4OH dissolution from BP4OLi/CMK-3 electrode could be observed by the naked eye (inset of **Figure 3a**). For comparison, the BP4OH/SP electrode only showed unsatisfactory specific capacity of ~216 mAh g<sup>-1</sup> at the 30<sup>th</sup> cycle (50 mA g<sup>-1</sup>). The rate performance of the BP4OLi/CMK-3 electrode was shown in **Figure 3c**. At the current densities of 100/200/300/400 mA g<sup>-1</sup>, the BP4OLi/CMK-3 electrode could realize the specific capacities of ~298/250/225/210 mAh g<sup>-1</sup>, respectively. At the high current density of 500 mA g<sup>-1</sup>, the capacity value of the BP4OLi/CMK-3 electrode still remained to be ~198 mAh g<sup>-1</sup>. The long-cycle profile of the BP4OLi/CMK-3 electrode was depicted in **Figure 3d**. And the average capacity of ~155 mAh g<sup>-1</sup> for the BP4OLi/CMK-3 electrode was realized during 600 cycles at the high current density of 500 mA g<sup>-1</sup>.

### 3.3 Oxidation→reduction cycle

#### 3.3.1 CV test

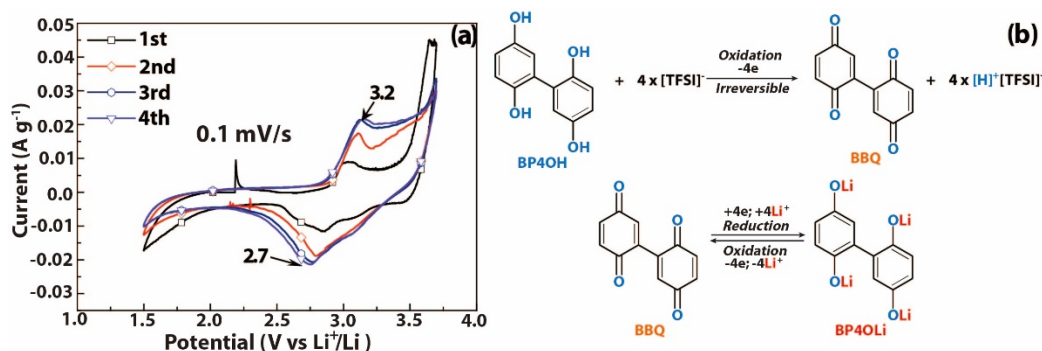


**Figure 4.** (a) CV curves of BP4OH by oxidation→reduction process. The scan rate was 0.1 mV s<sup>-1</sup>. The voltage window was 1.5–3.7 V; (b) The detailed mechanism of BP4OH by oxidation→reduction process in Li-ion cells.

Based on the previous study, BP4OH can be oxidized to 2,2'-bis(1,4-benzoquinone) (BBQ) by chemical oxidants. Herein, we initially proved that BP4OH can also be in-situ oxidized to BBQ on Al foil through electrochemical route. To confirm our hypothesis, the CV test was carried out by setting oxidation to 3.7 V during the 1<sup>st</sup> cycle. Therefore, the anodic scan was starting from 1.5–3.7 V (vs. Li<sup>+</sup>/Li) in the 1<sup>st</sup> cycle. And this procedure was called oxidation→reduction cycle. As shown in **Figure 4a**, it was impressive that a distinctive anodic peak (oxidation peak) located at ~3.1 V could appear for the BP4OH electrode in the 1<sup>st</sup> cycle. More importantly, its back reduction process was reversible and appeared at ~2.8 V. At the same time, in the following cycles, the two redox peaks were stable and located at ~3.2/2.7 V, respectively. Therefore, the detailed mechanism for this process could be summarized in **Figure 4b**. During the 1<sup>st</sup> oxidation scan, BP4OH could be oxidized to BBQ by electrochemical process on Al foil, along with the release of four equivalents of active proton (H<sup>+</sup>). Subsequently, BBQ and its reduced state (BP4OLi) played the redox couple for the following scans.

### 3.3.2 Li-ion half cells

The selected charge-discharge curves for the resulting BBQ electrode were shown in **Figure 5a**. The discharge capacity in the 1<sup>st</sup> cycle for the BBQ electrode was 473 mAh g<sup>-1</sup>, also quite close to

the theoretical capacity of BBQ ( $C_T=501 \text{ mAh g}^{-1}$ ). As shown in **Figure 5b**, the resulting BBQ electrode fulfilled the average capacity of  $\sim 204 \text{ mAh g}^{-1}$  during 100 cycles and remained  $\sim 160 \text{ mAh g}^{-1}$  @100<sup>th</sup> cycle under the low current density of  $50 \text{ mA g}^{-1}$ . The rate performance of the BBQ electrode was shown in **Figure 5c**. At the current densities of 100/200/300/400  $\text{mA g}^{-1}$ , the specific capacities of the BBQ electrode were  $\sim 298/250/225/210 \text{ mAh g}^{-1}$ , respectively. And at the high current density of  $500 \text{ mA g}^{-1}$ , the capacity value of the BBQ electrode still remained to be  $\sim 204 \text{ mAh g}^{-1}$ . The long-cycle profile of the BBQ electrode was also depicted in **Figure 5d**. And the average capacity value realized for the BBQ electrode was  $\sim 101 \text{ mAh g}^{-1}$  during 600 cycles at the high current density of  $500 \text{ mA g}^{-1}$ .

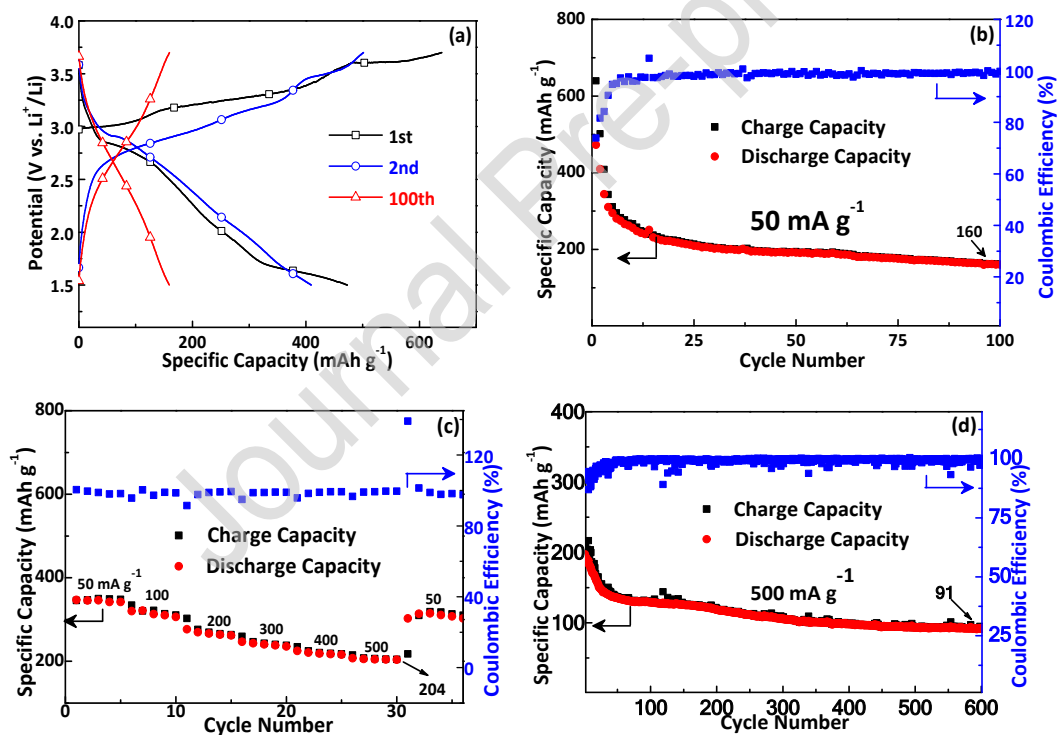


**Figure 5.** (a) The selected charge-discharge curves for the BBQ electrode by the oxidation→reduction process; (b) The 100 cycles for the BBQ electrode at  $50 \text{ mA g}^{-1}$ ; (c) The rate performance of the BBQ electrode; (d) The 600 cycles for the BBQ electrode at  $500 \text{ mA g}^{-1}$ .

### 3.4 Two-case comparisons

#### 3.4.1 Cell stability

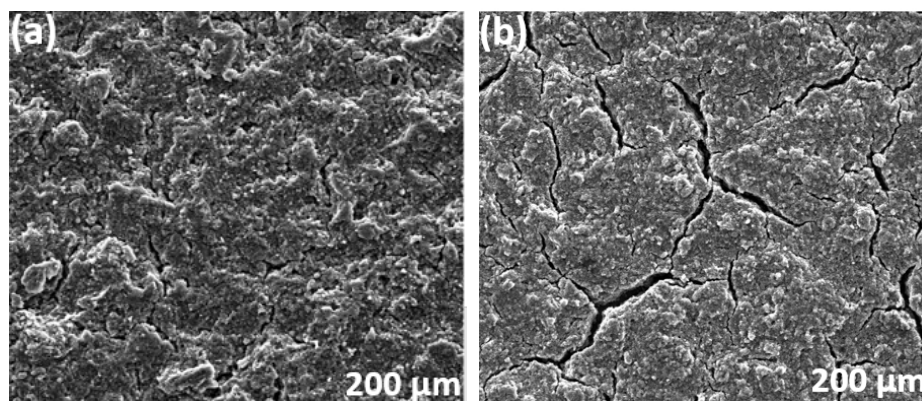


**Figure 6.** The SEM images for (a) BP4OH/CMK-3 electrode by reduction→oxidation cycle; (b) BP4OH/CMK-3 electrode by oxidation→reduction cycle.

By detailed comparisons, it seemed that the reduction→oxidation case of BP4OH could exhibit better cell stability than the oxidation→reduction case in Li-ion half cells ( $120 \text{ mAh g}^{-1}$  vs.  $91 \text{ mAh g}^{-1}$  @600<sup>th</sup> cycle). As shown by the scanning electron microscopy (SEM) images, the BP4OH/CMK-3 electrode with the reduction→oxidation process after cycling displayed a smooth and intense surface (**Figure 6a**) while the oxidation→reduction one (**Figure 6b**) showed the obvious large cracks on the surface. Therefore, the intense surface for the reduction→oxidation case may be indicative of the formation of thick solid-electrolyte interface (SEI) under low reduction potential [30, 31]. And the SEI could be protective to the dissolution of organic redox materials, thus leading to its better cycle stability. As further confirmed by the EIS tests after cycling in **Figure 7**, a small semicircle could appear in the real axis of high frequency for the reduction→oxidation case (inset of **Figure 7a**) when compared to the oxidation→reduction one (inset of **Figure 7b**), which was clearly indicative of SEI formation [30, 31].

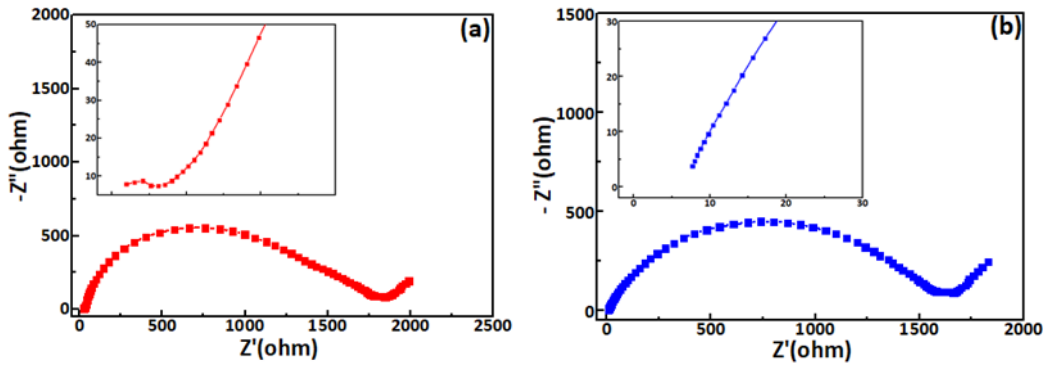


**Figure 7.** The EIS tests for BP4OH/CMK-3 electrode. (a) BP4OH/CMK-3 electrode by reduction→oxidation cycle; (b) BP4OH/CMK-3 electrode by oxidation→reduction cycle.

### 3.4.2 Li-ion diffusion

On the other hand, it seemed that both the reduction→oxidation case and the oxidation→reduction case exhibited the similar rate performance (198 mAh g<sup>-1</sup> vs. 204 mAh g<sup>-1</sup>@500 mA g<sup>-1</sup>). Consequently, the GITT tests were carried out to compare Li<sup>+</sup> diffusion coefficient for two cases.

$$D_{Li^+} = \frac{4}{\pi} \left( \frac{n_m V_m}{S} \right)^2 \left( \frac{\Delta E_s}{\tau (dE_\tau / d\sqrt{\tau})} \right)^2 = \frac{4}{\pi} \left( \frac{V}{S} \right)^2 \left( \frac{\Delta E_s}{\tau (dE_\tau / d\sqrt{\tau})} \right)^2 \approx \frac{4}{\pi \tau} (L)^2 \left( \frac{\Delta E_s}{\Delta E \tau} \right)^2$$

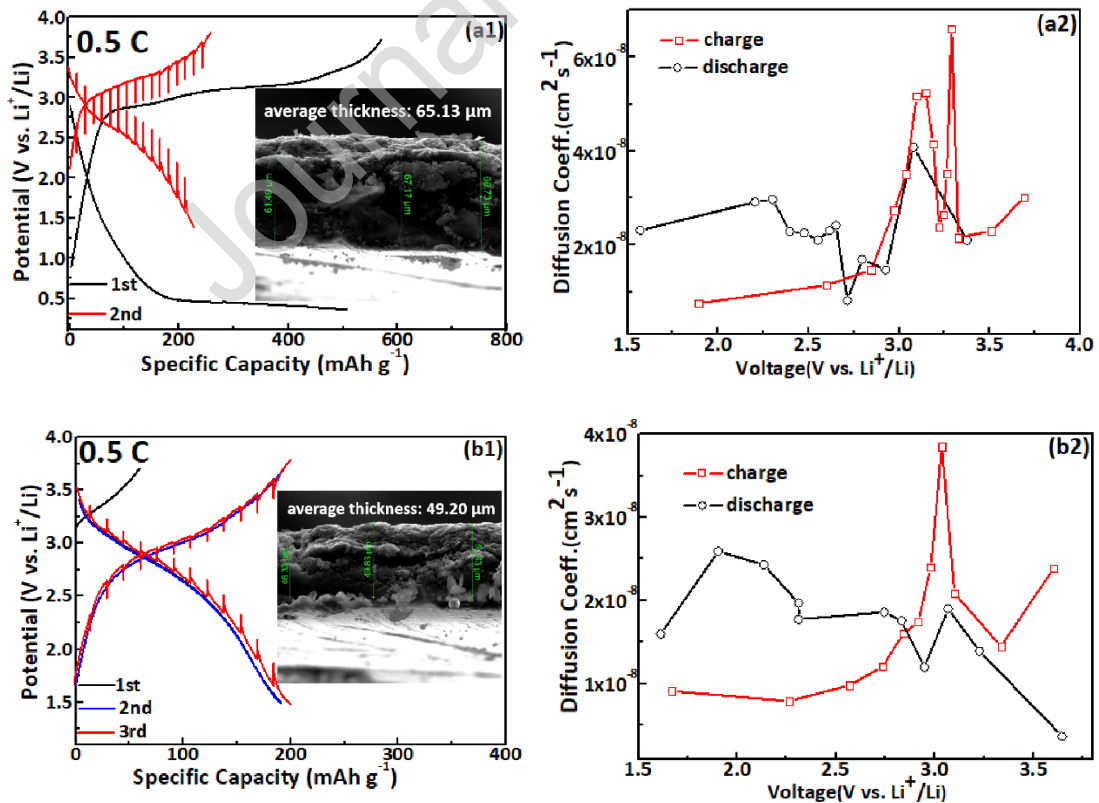


**Figure 8.** The GITT curves and the realized Li-ion diffusion coefficient for (a) BP4OH/CMK-3 electrode by reduction→oxidation process; (b) BP4OH/CMK-3 electrode by oxidation→reduction process.

According to the above formula, the GITT curves were measured by using a constant current density of 0.5 C for 5 min and then resting for 10 min at open circuit (1 C corresponds to the current density of 443 mA g<sup>-1</sup>) [32, 33]. And in the above formula,  $\pi$  is 3.14;  $\tau$  is 600s (10 min);  $L$  is the average electrode thickness measured by SEM images (inset of **Figure 8a1** and **b1**);  $\Delta E_s$  is potential difference between the previous relaxation and the current relaxation;  $\Delta E_t$  is potential difference before and after each constant current. The GITT curves and the obtained results for two cases were shown in **Figure 8a2** and **b2**, respectively. As expected, the electrode with the reduction→oxidation cycle showed similar Li-ion diffusion coefficient ( $\sim 2.74 \times 10^{-8} \text{ cm}^2 \text{ s}^{-1}$ ) with the oxidation→reduction one ( $\sim 1.88 \times 10^{-8} \text{ cm}^2 \text{ s}^{-1}$ ). Therefore, from the EIS and GITT results, it was confirmed that the BP4OH/CMK-3 electrode with different electrochemical pathways could still show the similar electron and ion conductivity.

#### 4. Conclusions

In summary, a small organic molecule of 2,2',5,5'-tetrahydroxybiphenyl (BP4OH) is exploited as the new organic cathode for Li-ion batteries. For the first time, we demonstrate that the redox states of BP4OH can be well in-situ manipulated on Al foil. For example, by reducing in the 1<sup>st</sup> cycle (reduction→oxidation), its related lithium 2,2'-bis[benzene-1,4-bis(olate)] (BP4OLi) is formed on Al foil. By oxidizing in the 1<sup>st</sup> cycle (oxidation→reduction), BP4OH can be oxidized to 2,2'-bis(1,4-benzoquinone) (BBQ). Both formed BP4OLi and BBQ are proved to be active in the following battery tests. This work reveals very interesting redox behaviors for organic electrodes.

#### Acknowledgements

This work is supported by the National Natural Science Foundation of China (51603028), the Fundamental Research Funds of UESTC (ZYGX2019J027) and the National Key Specialty Construction Project of Clinical Pharmacy (30305030698).

### Conflict of interest

The authors declare no conflict of interest.

### REFERENCES

- [1] J. Xie, Q. Zhang, Recent progress in rechargeable lithium batteries with organic materials as promising electrodes, *J. Mater. Chem. A*, 4 (2016) 7091-7106.
- [2] A. Jouhara, N. Dupre, A.-C. Gaillot, D. Guyomard, F. Dolhem, P. Poizot, Raising the redox potential in carboxyphenolate-based positive organic materials via cation substitution, *Nat. Commun.*, 9 (2018) 4401.
- [3] Y. Lu, X. Hou, L. Miao, L. Li, R. Shi, L. Liu, J. Chen, Cyclohexanone with Ultrahigh Capacity as Cathode Materials for Lithium-Ion Batteries, *Angew. Chem. Int. Ed.*, 58 (2019) 7020-7024.
- [4] W. Walker, S. Grugeon, O. Mentre, S. Laruelle, J.-M. Tarascon, F. Wudl, Ethoxycarbonyl-Based Organic Electrode for Li-Batteries, *J. Am. Chem. Soc.*, 132 (2010) 6517-6523.
- [5] M. Armand, S. Grugeon, H. Vezin, S. Laruelle, P. Ribiere, P. Poizot, J.M. Tarascon, Conjugated dicarboxylate anodes for Li-ion batteries, *Nat. Mater.*, 8 (2009) 120-125.
- [6] X. Han, C. Chang, L. Yuan, T. Sun, J. Sun, Aromatic carbonyl derivative polymers as high-performance Li-ion storage materials, *Adv. Mater.*, 19 (2007) 1616.
- [7] L.C. Miao, L.J. Liu, Z.F. Shang, Y.X. Li, Y. Lu, F.Y. Cheng, J. Chen, The structure-electrochemical property relationship of quinone electrodes for lithium-ion batteries, *Phys. Chem. Chem. Phys.*, 20 (2018) 13478-13484.
- [8] S.A. Khan, S. Ali, K. Saeed, M. Usman, I. Khan, Advanced cathode materials and efficient electrolytes for rechargeable batteries: practical challenges and future perspectives, *J. Mater. Chem. A*, 7 (2019) 10159-10173.
- [9] Z. Song, Y. Qian, T. Zhang, M. Otani, H. Zhou, Poly(benzoquinonyl sulfide) as a High-Energy Organic Cathode for Rechargeable Li and Na Batteries, *Adv. Sci.*, 2 (2015) 1500124.
- [10] Y. Liang, Y. Jing, S. Gheyhani, K.-Y. Lee, P. Liu, A. Facchetti, Y. Yao, Universal quinone electrodes for long cycle life aqueous rechargeable batteries, *Nat. Mater.*, 16 (2017) 841.
- [11] M. Miroshnikov, K.P. Divya, G. Babu, A. Meiyazhagan, L.M.R. Arava, P.M. Ajayan, G. John, Power from nature: designing green battery materials from electroactive quinone derivatives and organic polymers, *J. Mater. Chem. A*, 4 (2016) 12370-12386.
- [12] M.E. Bhosale, S. Chae, J.M. Kim, J.-Y. Choi, Organic small molecules and polymers as an electrode material for rechargeable lithium ion batteries, *J. Mater. Chem. A*, 6 (2018) 19885-19911.
- [13] T. Ma, Q. Zhao, J. Wang, Z. Pan, J. Chen, A Sulfur Heterocyclic Quinone Cathode and a Multifunctional Binder for a High-Performance Rechargeable Lithium-Ion Battery, *Angew. Chem. Int. Ed.*, 55 (2016) 6428-6432.
- [14] A.E. Lakraychi, E. Deunf, K. Fahsi, P. Jimenez, J.P. Bonnet, F. Djedaini-Pilard, M. Becuwe, P. Poizot,

F. Dolhem, An air-stable lithiated cathode material based on a 1,4-benzenedisulfonate backbone for organic Li-ion batteries, *J. Mater. Chem. A*, 6 (2018) 19182-19189.

[15] Z. Song, H. Zhou, Towards sustainable and versatile energy storage devices: an overview of organic electrode materials, *Energy Environ. Sci.*, 6 (2013) 2280-2301.

[16] J.B. Goodenough, Y. Kim, Challenges for Rechargeable Li Batteries, *Chem. Mat.*, 22 (2010) 587-603.

[17] M.S. Whittingham, Lithium batteries and cathode materials, *Chem. Rev.*, 104 (2004) 4271-4301.

[18] S.W. Wang, L.J. Wang, K. Zhang, Z.Q. Zhu, Z.L. Tao, J. Chen, Organic  $\text{Li}_4\text{C}_8\text{H}_2\text{O}_6$  Nanosheets for Lithium-Ion Batteries, *Nano Lett.*, 13 (2013) 4404-4409.

[19] Y. Hu, W. Tang, Q. Yu, C. Yang, C. Fan, In Situ Electrochemical Synthesis of Novel Lithium-Rich Organic Cathodes for All-Organic Li-Ion Full Batteries, *ACS Appl. Mater. Interfaces*, 11 (2019) 32987-32993.

[20] C. Wang, W. Tang, Z. Yao, Y. Chen, J. Pei, C. Fan, Using an organic acid as a universal anode for highly efficient Li-ion, Na-ion and K-ion batteries, *Org. Electron.*, 62 (2018) 536-541.

[21] G. Sartori, R. Maggi, F. Bigi, A. Arienti, G. Casnati, Oxidative coupling of dichloroaluminium phenolates: Highly selective synthesis of hydroxylated Bi- and tetraaryls, *Tetrahedron*, 48 (1992) 9483-9494.

[22] R.J. Bushby, D.R. McGill, K.M. Ng, N. Taylor, p-Doped high spin polymers, *J. Mater. Chem.*, 7 (1997) 2343-2354.

[23] C. Wang, W. Tang, Z. Yao, B. Cao, C. Fan, Potassium perylene-tetracarboxylate with two-electron redox behaviors as a highly stable organic anode for K-ion batteries, *Chem. Commun.*, 55 (2019) 1801-1804.

[24] H. Li, W. Duan, Q. Zhao, F. Cheng, J. Liang, J. Chen, 2,2'-Bis(3-hydroxy-1,4-naphthoquinone)/CMK-3 nanocomposite as cathode material for lithium-ion batteries, *Inorg. Chem. Front.*, 1 (2014) 193-199.

[25] S. Jun, S.H. Joo, R. Ryoo, M. Kruk, M. Jaroniec, Z. Liu, T. Ohsuna, O. Terasaki, Synthesis of new, nanoporous carbon with hexagonally ordered mesostructure, *J. Am. Chem. Soc.*, 122 (2000) 10712-10713.

[26] W. Tang, H. He, J. Shi, B. Cao, C. Yang, C. Fan, Poly (N-vinylcarbazole)(PVK) as a high-potential organic polymer cathode for dual-intercalation Na-ion batteries, *Org. Electron.*, 75 (2019) 105386.

[27] Z. Yao, W. Tang, X. Wang, C. Wang, C. Yang, C. Fan, Synthesis of 1, 4-benzoquinone dimer as a high-capacity ( $501 \text{ mA hg}^{-1}$ ) and high-energy-density ( $> 1000 \text{ Wh kg}^{-1}$ ) organic cathode for organic Li-Ion full batteries, *J. Power Sources*, 448 (2020) 227456.

[28] C. Guo, K. Zhang, Q. Zhao, L. Peia, J. Chen, High-performance sodium batteries with the 9,10-anthraquinone/CMK-3 cathode and an ether-based electrolyte, *Chem. Commun.*, 51 (2015) 10244-10247.

[29] W. Xiong, W. Huang, M. Zhang, P. Hu, H. Cui, Q. Zhang, Pillar 5 quinone-Carbon Nanocomposites as High-Capacity Cathodes for Sodium-Ion Batteries, *Chem. Mat.*, 31 (2019) 8069-8075.

[30] J. Guo, X. Du, X. Zhang, F. Zhang, J. Liu, Facile Formation of a Solid Electrolyte Interface as a Smart Blocking Layer for High-Stability Sulfur Cathode, *Adv. Mater.*, 29 (2017) 1700273.

[31] J. Zheng, M. Gu, H. Chen, P. Meduri, M.H. Engelhard, J.-G. Zhang, J. Liu, J. Xiao, Ionic liquid-enhanced solid state electrolyte interface (SEI) for lithium-sulfur batteries, *J. Mater. Chem. A*, 1 (2013) 8464-8470.

[32] C. Yang, J. Chen, X. Ji, T.P. Pollard, X. Lu, C.-J. Sun, S. Hou, Q. Liu, C. Liu, T. Qing, Y. Wang, O. Borodin, Y. Ren, K. Xu, C. Wang, Aqueous Li-ion battery enabled by halogen conversion-intercalation chemistry in graphite, *Nature*, 569 (2019) 245.

[33] M. Mao, X. Ji, S. Hou, T. Gao, F. Wang, L. Chen, X. Fan, J. Chen, J. Ma, C. Wang, Tuning Anionic Chemistry To Improve Kinetics of Mg Intercalation, Chem. Mat., 31 (2019) 3183-3191.

Journal Pre-proof

Declaration of Interest Statement: The authors declare no conflict of interest.

Journal Pre-proof

### Highlights:

1. A new organic cathode of 2,2',5,5'-tetrahydroxybiphenyl (BP4OH) is reported.
2. BP4OH can in-situ get reduced to BP4OLi in Li-ion cells.
3. Average capacity of 155 mAh g<sup>-1</sup> for BP4OLi is realized for 600 cycles.
4. BP4OH can in-situ get oxidized to 2,2'-bis(1,4-benzoquinone) (BBQ).
5. Average capacity of 101 mAh g<sup>-1</sup> for BBQ is obtained for 600 cycles.

Journal Pre-proof